

Article

# High Quality Syngas Production with Supercritical Biomass Gasification Integrated with a Water–Gas Shift Reactor

M. M. Sarafraz <sup>1</sup>, Mohammad Reza Safaei <sup>2,3,\*</sup>, M. Jafarian <sup>1</sup>, Marjan Goodarzi <sup>4,5,\*</sup> and M. Arjomandi <sup>1</sup>

<sup>1</sup> School of Mechanical Engineering, University of Adelaide, Adelaide, Australia

<sup>2</sup> Division of Computational Physics, Institute for Computational Science, Ton Duc Thang University, Ho Chi Minh City, Vietnam

<sup>3</sup> Faculty of Electrical and Electronics Engineering, Ton Duc Thang University, Ho Chi Minh City, Vietnam

<sup>4</sup> Department of Mechanical Engineering, Lamar University, Beaumont, TX 77705, USA

<sup>5</sup> Sustainable Management of Natural Resources and Environment Research Group, Faculty of Environment and Labour Safety, Ton Duc Thang University, Ho Chi Minh City, Vietnam

\* Correspondence: cfd\_safaei@tdtu.edu.vn (M.R.S.); mgoodarzi@lamar.edu or marjan.goodarzi@tdtu.edu.vn (M.G.)

Received: 30 May 2019; Accepted: 1 July 2019; Published: 5 July 2019



**Abstract:** A thermodynamic assessment is conducted for a new configuration of a supercritical water gasification plant with a water–gas shift reactor. The proposed configuration offers the potential for the production of syngas at different H<sub>2</sub>:CO ratios for various applications such as the Fischer–Tropsch process or fuel cells, and it is a path for addressing the common challenges associated with conventional gasification plants such as nitrogen dilution and ash separation. The proposed concept consists of two reactors, R<sub>1</sub> and R<sub>2</sub>, where the carbon containing fuel is gasified (in reactor R<sub>1</sub>) and in reactor R<sub>2</sub>, the quality of the syngas (H<sub>2</sub>:CO ratio) is substantially improved. Reactor R<sub>1</sub> is a supercritical water gasifier and reactor R<sub>2</sub> is a water–gas shift reactor. The proposed concept was modelled using the Gibbs minimization method with HSC chemistry software. Our results show that the supercritical water to fuel ratio (SCW/C) is a key parameter for determining the quality of syngas (molar ratio of H<sub>2</sub>:CO) and the carbon conversion reaches 100%, when the SWC/C ratio ranges between two and 2.5 at 500–1000 °C.

**Keywords:** supercritical water gasification; water–gas shift reactor; biomass gasification; syngas quality

## 1. Introduction

The energy crisis and environmental pollution due to the combustion of carbon-containing fuels have resulted in more research being conducted on renewable energy and clean energy resources as potential alternatives to fossil fuels [1–3]. Synthetic gas (syngas) is a mixture of hydrogen and carbon monoxide, which is a promising replacement for fossil fuels. It is a cheap, clean burning fuel, easy-to-transport gas, and has a wide range of applications such as some types of fuel cell systems [4,5] and the Fischer–Tropsch process [4]. Therefore, it has received ever-increasing special attention throughout the past decades. Gasification is the common pathway to produce syngas from carbonaceous fuels. In conventional air-blown gasification systems, air is used for the partial oxidation of fuel, which not only adds impurities (e.g., sulphur dioxide) to the final gaseous products but supplies nitrogen to the syngas, which reduces the quality of the syngas product. One plausible solution for this challenge is to use oxy-fuel gasifiers to avoid the appearance of impurities and nitrogen at the

outlet, which in turn adds to the cost and complexity of the process. Therefore, there is a need to seek alternatives that produce high quality syngas, while addressing the aforementioned challenges [5].

Chemical looping gasification is an emerging technology for the production of syngas using a solid oxygen carrier (OC). This technology addresses the nitrogen dilution but also has the potential to reduce and/store greenhouse gases (GHG) such as CO<sub>2</sub>. In this concept, two interconnected reactors, the gasifier and the air reactor, are employed. In the gasifier, metal oxides are reduced, and fuel is partially oxidized [6]. Syngas is the main product of the gasifier. Then, the reduced metal oxides are transported to the air reactor where particles of oxygen are recovered [7]. Notwithstanding the advantages of the solid oxygen carrier particles, there are some challenges associated with the use of the solid oxygen carriers in chemical looping systems. These include agglomeration and sintering [6,8–16], and also the need to separate the OC particles from any carry-over particles from the gasifier, as well as manage the deposition of carbon and ash on the OC particles [17]. These challenges significantly reduce the effectiveness of the oxygen carrier particles to transport oxygen between the reactors [16,18–22] and hence decreases the efficiency of the process [6]. However, this emerging concept is in the early stage of development and needs further investigation to understand its shortcomings. For example, a material constraint due to the sintering, breakage, and corrosion of metals, is one of the challenges associated with the use of molten metal in the chemical looping process.

One promising method to gasify a carbonaceous fuel is supercritical water (SCW) gasification. This concept offers a wide range of benefits over the other concepts such as:

- Supercritical water has zero surface tension and most of the carbon-containing fuels are soluble in it, and therefore diffusion and penetration of water in the carbon with insignificant mass transfer resistance is plausible [23];
- The SCW gasification process is flexible with respect to the type of the carbonaceous fuel. For example, different types of biomass, coal, or even municipal waste with various contents of moisture and impurities are used as fuel sources [24];
- The required operating temperature for the gasification lies between 400 °C and 1000 °C depending on the type of the fuel and quality of the syngas;
- The produced carbon dioxide easily separates from H<sub>2</sub> using pressurized water;
- Some physical properties of water, such as density, ion product, dielectric constant, viscosity, diffusivity, and solubility, change near or at its thermodynamic critical point (T = 374 °C and P = 22.1 MPa). At the critical point, water behaves similar to a dense gas with a consequent removal of any interphase mass transport processes. Organic compounds have high solubilities and complete miscibility with supercritical water [25];
- The process is high pressure, which reduces the costs related to the storage of the gaseous products such as post-compression operation.

These advantages provide plausible conditions for better gasification of carbonaceous fuel, particularly biomass in supercritical water. For example, thermodynamic assessment and system modelling for the gasification of biomass with supercritical water were conducted by Withag et al. [26]. The selected feedstock was a wet biomass comprised of 70% water by weight. It was shown that the gasification is feasible without any further drying process. Thermochemical equilibrium analysis was used for the modelling of the process and it was found that the composition of the product gases could be tailored to the desired product composition by changing the process parameters such as the reactor temperature, pressure, and the concentration of organic material in the feed. However, the pressure of the reactor was 100–300 bar, which was technically challenging and expensive. In addition, the proposed system produced 38% CO<sub>2</sub>, which was one main challenge of the supercritical gasification at higher temperatures.

In another work, Guan et al. [27] investigated the gasification of algae nanochloropsis in supercritical water and showed that with an increase in the temperature of the gasifier, more carbon dioxide is produced. By reducing the operating temperature of the gasifier, the mole fraction of

CO<sub>2</sub> slightly decreased, however, the quality of the produced synthetic gas (H<sub>2</sub>:CO molar ratio) was low. A similar trend was reported in the gasification of dry starch as biomass conducted by Yakaboylu et al. [28]. Thus, to achieve high quality syngas, there is a need to separate the CO<sub>2</sub> from other gaseous products. In a study conducted by Guo et al. [29], they reported the controversial result that operating temperature has a strong influence on the gasification of biomass with supercritical water such that the gasification efficiency and H<sub>2</sub> production at higher temperatures inverses the quantity of the CO<sub>2</sub> product [29]. Thus, further investigation on the role of temperature on the supercritical gasification of biomass and mole fraction of gaseous products is required.

The diversity of components in gaseous products obtained by the gasification pathway has also been a popular subject of research, because carbon-containing fuels such as biomass have different compositions of cellulose, glucose, glycerol, lignin, and phenolic which may result in a substantial change in the gasification reactions and consequently changes the configuration of the reactor [29–31]. For example, Guo et al. [32] performed an experimental investigation on the catalytic and noncatalytic supercritical gasification of glycerol in a tubular quartz reactor for hydrogen production. They showed that by using a catalyst, the main gaseous products are hydrogen with the mole fraction of 59%, followed by CO<sub>2</sub> with the mole fraction of 29.9%, CH<sub>4</sub> with the mole fraction of ~6.5%, and CO with the mole fraction of ~4.5%. Noticeably, in the absence of the nickel catalyst, the mole fraction of hydrogen decreased to 50%, the mole fraction of CO<sub>2</sub> decreased to 24.93%, and the mole fraction of CO decreased to 21.13%. Therefore, depending on the type of feedstock, a specific type of the reactor or configuration of the process is required [33–35].

For example, one potential configuration for supercritical gasification is a fluidized bed system. In a study conducted by Lu et al. [36], the hydrodynamic behavior of a supercritical gasifier was evaluated at temperatures ranging from 360 °C to 420 °C and pressure ranging from 23 MPa to 27 MPa. They identified that a double symmetric feeding pipe with an angle of 45° provided uniform solid distribution and a long residence time, which potentially also represented better chemical efficiency. However, it was identified that depending on the composition of the feedstock, the configuration of the system might need a major modification in order to produce high-quality syngas [33]. Hence, in our research, the thermodynamic potential for a new configuration that would produce a high quality syngas with supercritical water is investigated for graphite (pure carbon) as a surrogate for any carbonaceous fuel and biomass. The presence of the water–gas shift reactor removes the barrier of dependence of the configuration of supercritical gasification on the composition of feedstock. Thus, the proposed gasification plant is combined with a water–gas shift (WGS) reactor to control the H<sub>2</sub>:CO ratio. The influence of different operating conditions, including the ratio of supercritical water to feedstock, temperature, and the pressure of the reactors on the gaseous products is investigated. The chemical performance of the proposed concept is investigated for three different biomass feedstocks.

## 2. Methodology

Figure 1 presents a schematic diagram of the operating conditions considered for this research. To apply the thermochemical equilibrium and sensitivity analysis, different temperatures and pressures were applied to reactors R<sub>1</sub> and R<sub>2</sub>. The minimum temperature and pressure to achieve the supercritical water was 374 °C and 25 bar, respectively, which were applied to reactor R<sub>1</sub>. For storing the syngas, it was plausible to pressurize the Reactor R<sub>2</sub>. A sensitivity analysis on the quality of the syngas and the temperature of reactor R<sub>2</sub> was conducted to identify the optimum range of the temperature for the reactor, which was between 500 °C and 800 °C. At this range of temperature, the mole fraction of CO<sub>2</sub> and methane was also minimized, which increased the quality of the syngas. In this research, a syngas quality (H<sub>2</sub>:CO molar ratio) greater than 2 was the target value of the simulation, which potentially has a wide range of applications in gas to liquid processes, transportation fuels, the Fischer–Tropsch process, and fuel cells. Thus, the last stage was to remove any moisture content from the syngas using a refrigerant cooler.

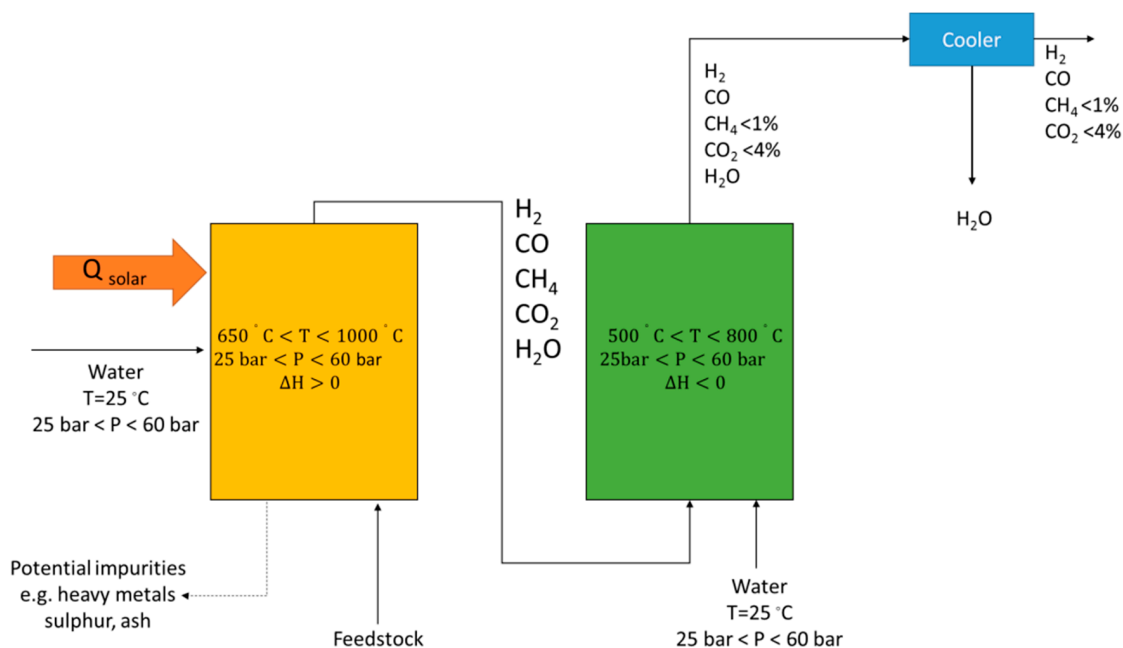


Figure 1. Detailed operating conditions of the process for supercritical synthetic gas (syngas) production.

Figure 2 presents a schematic diagram of the water supercritical gasification, consisting of two reactors namely the supercritical gasifier (R<sub>1</sub>) and the WGS reactor (R<sub>2</sub>). To efficiently use the released heat from the exothermic reactions in the gasifier (methanation and WGS reactions), both water (stream 1), and fuel (stream 2) were fed into the supercritical gasifier (reactor R<sub>1</sub>).

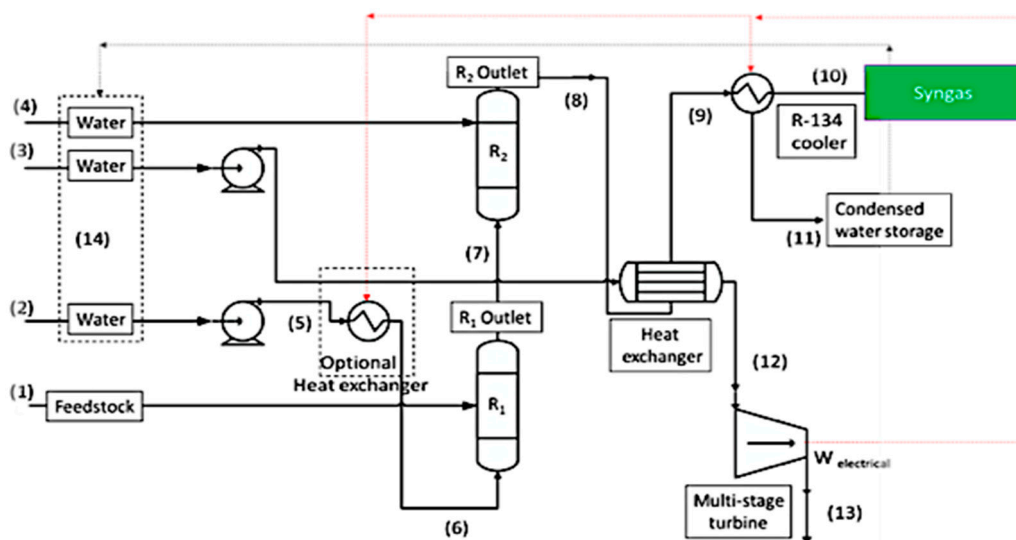


Figure 2. Schematic diagram of the supercritical gasification.

To enhance the quality of syngas (H<sub>2</sub>:CO molar ratio), the gaseous products from R<sub>1</sub> (stream 7) were fed into a WGS reactor (reactor R<sub>2</sub>). A cold water (stream 4) was fed into the reactor R<sub>2</sub> preceding the WGS reaction, which is exothermic and absorbs the released heat. The outlet from R<sub>2</sub> (stream 8) was fed into a heat exchanger to produce a high-pressure steam (stream 12) from the cold water pumped into the heat exchanger (stream 3). The generated high-pressure steam was then fed into a two-stage steam turbine to produce ~11% of the total input energy to be used as electrical power for work in the plant. Then, the cold syngas from the heat exchanger (stream 10) was stored for further use. Notably, to the best of our knowledge there is no industrial WGS reaction, or any demonstration of it, which

operate at the proposed conditions yet. However, the scope of this work is to thermodynamically assess the potential of the proposed system for high quality syngas production and an investigation on this subject is beyond the scope of the present investigation.

To predict the potential reactions occurring in the reactors, the Gibbs minimization method [37–39] was employed. To achieve this, the Aspen Plus RGibbs reactor and HSC chemistry were used to estimate the Gibbs free energy of the potential reactions. To solve the model, the following assumptions were considered:

1. The reactions reach to the equilibrium;
2. Heat loss is negligible from all reactors, pipes, tanks, and units;
3. Heat and mass transfer coefficients are plausible to maintain the conditions for highest chemical performance of the reactions;
4. Graphite in the present work is a surrogate for more realistic feedstock, which is used in the Gibbs minimization simulation. Any impurities in the feedstock have a negligible influence on the reactions and only carbon reacts in the supercritical gasifier. If there is an impurity, it is completely separated in the form of ash from the supercritical gasifier due to the difference between the ash and supercritical water density;
5. The residence time is sufficient for the reactions to reach completion so that no unreacted carbon enters the WGS reactor;
6. No catalytic effect is considered in the modelling. However, metal oxides and some composites have been identified as a suitable heat and mass transfer medium [40–44], which can also improve the supercritical gasification reactions [45–47];
7. The process is isobar and the pressure of the reactors is the same.

Table 1 shows the potential reactions occurring in the proposed concept.

**Table 1.** Potential reactions of supercritical water with carbon.

No.	Name	Reaction
1	Reforming	$C + H_2O(g) \leftrightarrow H_2(g) + CO(g)$
2	Partial oxidation of graphite	$3C + 2H_2O(g) \leftrightarrow CH_4(g) + 2CO(g)$
3	Complete oxidation of graphite	$C + 2H_2O(g) \leftrightarrow 2H_2(g) + CO_2(g)$
4	Methanation	$C + 2H_2(g) \leftrightarrow CH_4(g)$
5	Water-gas shift reaction	$CO(g) + H_2O(g) \leftrightarrow H_2(g) + CO_2(g)$
6	Boudouard reaction	$CO_2(g) + C \leftrightarrow 2CO(g)$

To assess the chemical performance of the reactors, the following parameter is defined:

$$\frac{SCW}{C} = \frac{n_{steam}}{n_{feedstock}} \quad (1)$$

where,  $n_{steam}$  is the moles of supercritical steam required for the gasification and  $n_{feedstock}$  is the moles of feedstock fed into the reactor. SCW and C stand for supercritical water and carbon, respectively. The carbon conversion is also defined with the following equation:

$$x = \frac{n_{feedstock,initial} - n_{feedstock,remaining}}{n_{feedstock,initial}} \times 100 \quad (2)$$

where,  $n_{feedstock,initial}$  is the moles of feedstock introduced to the reactor and  $n_{feedstock,remaining}$  is the unreacted moles of carbon or feedstock. To perform the sensitivity analysis and to compare the results to a reference case, a reference condition is defined in Table 2.

To validate the results of the modelling, a comparison was made between the results obtained with the developed model and those reported in the literature. To make this comparison, the model

was validated using the same operating conditions given in the literature. The results of comparison showed that the estimated moles of production of hydrogen was similar to those reported in the literature [48–50]. As shown in Figure 3a, the moles of production of hydrogen estimated with the model is within the deviation of  $\pm 10\%$  of those of reported in the literature [51,52]. Likewise, the syngas quality ( $H_2:CO$  molar ratio), as presented in Figure 3b, was in good agreement with the literature with a deviation of  $\pm 15\%$ .

**Table 2.** Reference conditions used in the sensitivity analysis.

Parameter	T R1 (°C)	T R2 (°C)	Pressure (bar)	SCW/C
Range (min–max)	650–1000	500–800	25–60	0.01–3
Reference case	650	600	25	1

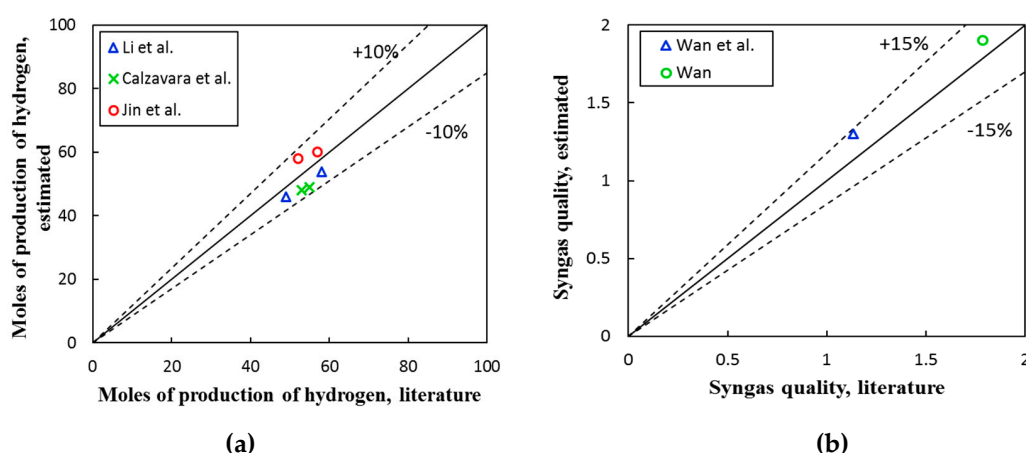


**Figure 3.** Validation of the model using the data reported in the literature, (a) comparison between estimated moles of production of hydrogen and data reported in previous works [48–50], (b) comparison between the estimated syngas quality ( $H_2:CO$  molar ratio) and those reported in the literature [51,52].

To assess the effect of biomass composition on the composition of the gas production, three different biomasses were selected from the literature. The proximate analysis and ultimate analysis of the biomasses are listed in Table 3. It is worth noting that most of the biomass have a very low sulphur content ( $<1\%$ ) and a high oxygen content ( $>35\%$ ). The content of sulphur considerably influences the quality of the syngas. The lower the sulphur content, the higher the quality of the syngas [53–55].

**Table 3.** Analysis of the agro biomass feedstock used in this research [56].

Feedstock	Proximate Analysis				Ultimate Analysis				
	Moisture Content	Ash	Volatile Matter	Fixed Carbon	C	H	N	S	O
Feedstock 1	55.31	60.32	30.32	9.36	22.3	3.3	2.1	0.5	11.3
Feedstock 2	47.98	40.24	34.55	25.21	50.2	3.8	2.7	0.5	2.4
Feedstock 3	41.39	52.67	32.19	15.14	37.8	3.1	2.3	0.42	3.6

### 3. Results and Discussion

#### 3.1. Gibbs Free Energy and Enthalpy Assessment

Figure 4a presents the dependence of the Gibbs free energy on the operating temperature of the gasifier and the WGS reactor for the different reactions listed in Table 1. As shown in Figure 3a, at  $T > 650$  °C, the Gibbs free energy for reactions 4 (methanation) and 5 (partial oxidation of graphite) is positive, meaning that these reactions are unlikely to occur at this temperature range. However,

the rest of the reactions occur within the gasifier and the WGS reactors. Therefore, for reactions to be spontaneous and feasible in the gasifier, the minimum temperature should be at least 650 °C, since over this temperature, the Gibbs free energy for reactions 1, 2, 3 and 6 is negative. Figure 4b presents the dependence of enthalpy of reactions on the temperature of the gasifier and the WGS reactors for the different reactions presented in Table 1 and shows that the enthalpy of the reactions does not significantly change with temperature and remains approximately constant. For example, for each of the reactions 1, 2, 3, and 6, the enthalpy of reaction remains constant at a temperature range between 650 °C and 1000 °C. It is worth noting that the total enthalpy of the reaction for the gasifier is endothermic and it is exothermic for the WGS reactor.

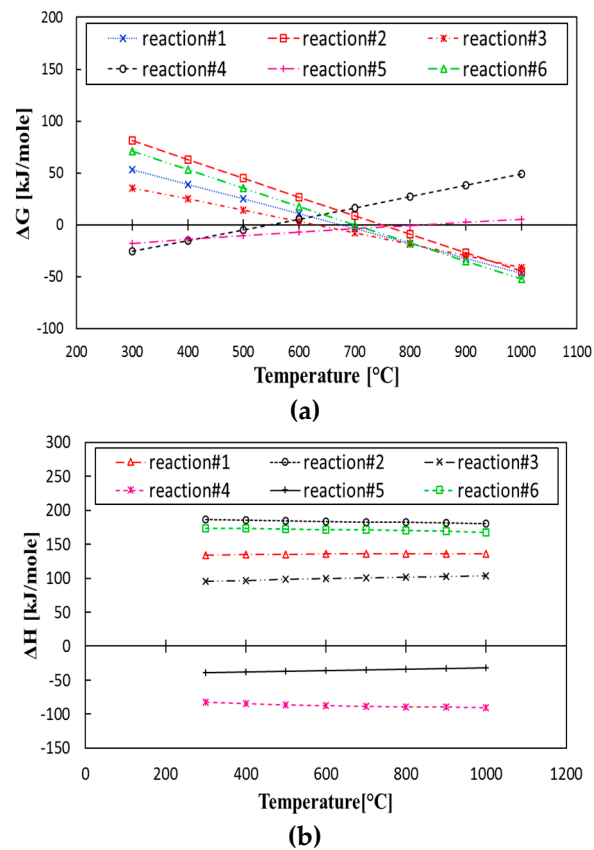
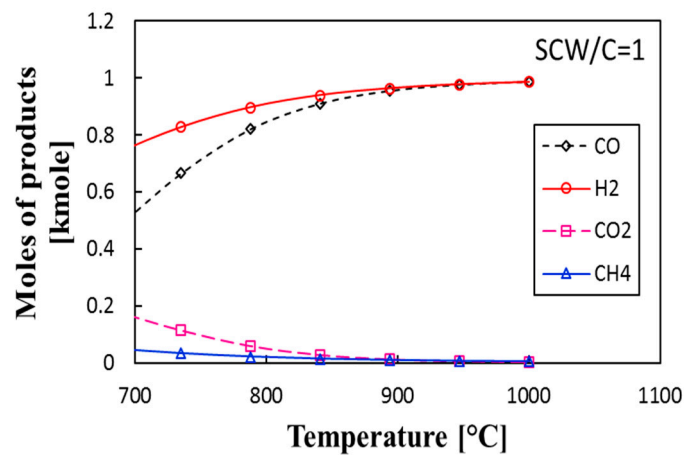


**Figure 4.** Dependence on temperature of the Gibbs free energy and enthalpy of the reaction with temperature. (a) Variation of the change in the Gibbs free energy of reactions with temperature for the reactions given in Table 1 and (b) variation of the enthalpy of the reaction with temperature for the reactions given in Table 1.

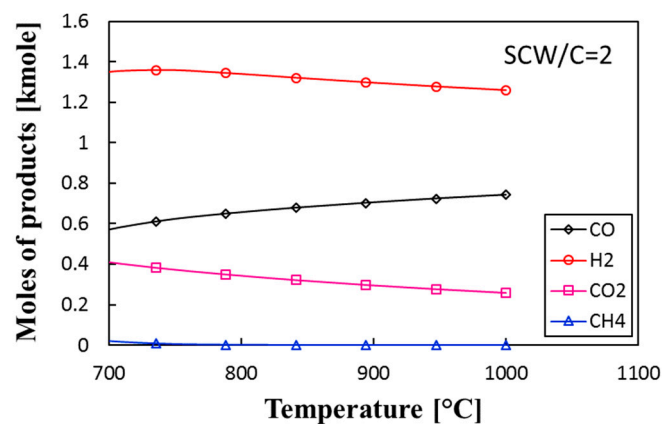
### 3.2. Thermochemical Equilibrium Assessment for Reactor $R_1$

Figure 5 presents the dependence of moles of gaseous products on the temperature of reactor  $R_1$  for the supercritical water to fuel ratio (SCW/C) = 1 at  $P = 25$  bar. It is worth noting that the supercritical water gasification occurs at operating pressures larger than 25 bar. For  $P < 25$  bar, the supercritical gasification does not occur, and the chemical conversion of carbon is very low. For an atmospheric gasification, more steam is required not only to enrich the hydrogen content but also to provide sufficient mixing in order to drive the reaction towards completion. We observe that with an increase in temperature the moles of production of  $H_2$  and CO increase. For example, at 700 °C, the mole fractions of  $H_2$  and CO are 0.86 kmol and 0.66 kmol, respectively. However, at  $T > 900$  °C, the mole fractions of  $H_2$  and CO are 0.99 kmol and 0.97 kmol, respectively. In addition, with an increase in temperature, the moles of production for  $CO_2$  and  $CH_4$  approaches zero. Importantly, this behaviour is only seen for an SCW/C ratio of one and smaller. For example, for the SCW/C = 2, as presented in

Figure 6, at 700 °C, the moles of production of H<sub>2</sub> and CO are 1.36 kmol and 0.54 kmol, respectively. In this case, the moles of production of CO<sub>2</sub> is 0.38 kmol, which slightly decreases with an increase in temperature. The moles of production of CO<sub>2</sub> at 1000 °C is 0.25 kmol. Importantly, an increase in temperature slightly decreases the production of hydrogen and increases the moles of production of CO, meaning that the quality of syngas (H<sub>2</sub>:CO molar ratio) slightly decreases. Therefore, the chemical performance of the reactor R<sub>1</sub> strongly depends on the molar ratio of SCW/C and is slightly dependent on the temperature of the reactor R<sub>1</sub>.

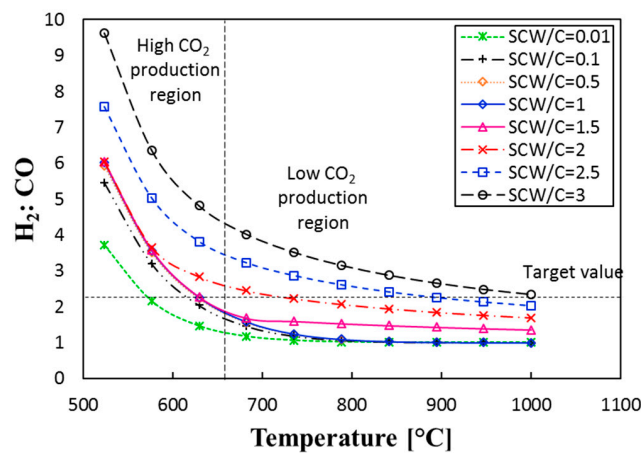


**Figure 5.** Variation of the mole fraction of the productions with temperature of the reactor R<sub>1</sub> at reference conditions given in Table 2.



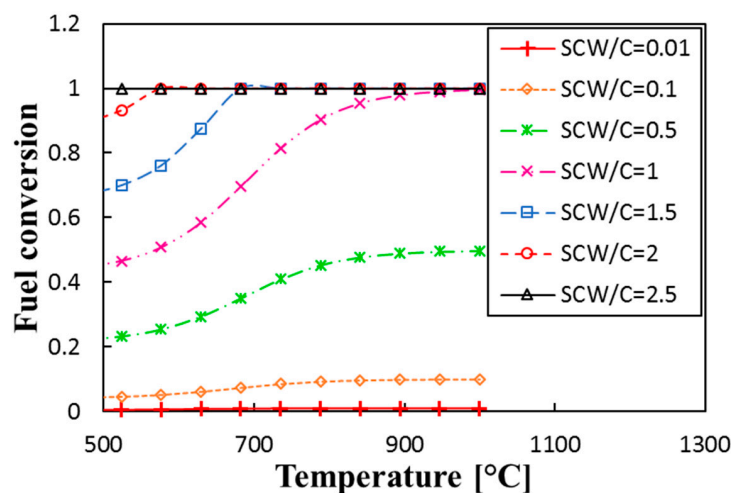
**Figure 6.** Variation of the mole fraction of the products with temperature at the reference condition in reactor at the supercritical water to fuel ratio (SCW/C) = 2.

Figure 7 presents the dependence of the molar ratio of H<sub>2</sub>:CO (referred to as syngas quality) on the temperature of reactor R<sub>1</sub> at the reference conditions. As shown in Figure 7, with an increase in the molar ratio of SCW/C, the quality of syngas (H<sub>2</sub>:CO molar ratio) increases, however, to achieve a target value of 2.1, a higher operating temperature is required. For example, at a molar ratio of SCW/C = 2, at T = 735 °C, the H<sub>2</sub>:CO molar ratio reached the target value, while for SCW/C = 3, the target value for the H<sub>2</sub>:CO molar ratio was satisfied at T = 988 °C. Moreover, with an increase in temperature, moles of production for CO<sub>2</sub> decreases, hence two different regimes are seen in Figure 7. Importantly, as shown in Figure 4a, the Gibbs free energy is negative for T > 650 °C, and therefore it is likely that the reactions proceed spontaneously in this range. Therefore, these two constraints limit the operating temperature of reactor R<sub>1</sub> between 650 °C and 900 °C. It is worth noting that at a large ratio of SCW/C, the energy requirement of the system is intensified as more steam is demanded for the supercritical reactor.



**Figure 7.** Variation of the syngas quality ( $H_2:CO$  molar ratio) with temperature, for different values of the supercritical water to fuel ratio ( $SCW/C$ ) in reactor  $R_1$ . The target (shown in the figure) is to obtain the syngas quality ( $H_2:CO$  molar ratio) value of  $\sim 2.1$ , suitable for the Fischer–Tropsch process and some fuel cell applications.

Figure 8 presents the dependence of fuel conversion on temperature for different molar ratios of  $SCW/C$ . As shown, with an increase in  $SCW/C$ , carbon conversion increases. For example, at  $700\text{ }^\circ\text{C}$ , for  $SCW/C = 0.01$ , the fuel conversion is only  $0.8\%$ , while for  $SCW/C = 1$ , it is  $69.8\%$ . Thus, the ratio of  $SCW/C$  strongly influences the fuel conversion. Likewise, with an increase in the temperature of the reactor, the fuel conversion increases, because with an increase in the value of  $SCW/C$ , the content of  $H_2O$  increases, which drives Equations (1)–(4) including gasification, partial oxidation of carbon, methanation, and complete oxidation of carbon. These reactions cause more carbon to be consumed and the value of the carbon conversion is promoted. For example, for  $SCW/C = 0.5$  and  $SCW/C = 1$ , at  $T = 800\text{ }^\circ\text{C}$  the fuel conversion is  $45\%$  and  $90\%$ , respectively, however, when the temperature is increased to  $1000\text{ }^\circ\text{C}$ , the fuel conversion reaches  $99.1\%$  and  $100\%$ , respectively. Therefore, it is estimated that graphite is completely converted into syngas at  $SCW/C > 1$  if the required temperature is maintained.



**Figure 8.** Variation of the carbon (fuel) conversion extent with temperature, for various values of  $SCW/C$  ratio in reactor  $R_1$ .

### 3.3. Thermochemical Equilibrium Assessment for Reactor $R_2$

Figure 9 presents the dependence of mole fraction of gaseous products on the temperature of reactor  $R_2$  for different components at  $P = 25\text{ bar}$ . As shown, with an increase in temperature, the mole fraction of  $H_2$  and  $CO$  increases. For example, at  $T = 800\text{ }^\circ\text{C}$ , the mole fractions of  $H_2$  and  $CO$  are  $0.49$

and 0.2, respectively, while at  $T = 1000\text{ }^{\circ}\text{C}$ , they are 0.61 and 0.31, respectively. Moreover, an increase in temperature decreases the mole fractions of  $\text{CO}_2$  and  $\text{CH}_4$ , respectively. For example, at  $700\text{ }^{\circ}\text{C}$ , the mole fractions of  $\text{CO}_2$  and  $\text{CH}_4$  are 0.2 and 0.18, respectively, while at  $1000\text{ }^{\circ}\text{C}$ , they are 0.04 and 0.01, respectively. Therefore, we conclude that at higher temperatures, the WGS reactor shows a better chemical performance. Notably, with an increase in the temperature of the water–gas shift reactor, the production of  $\text{CO}_2$  decreases since the water–gas shift reactor is an exothermic reactor and an increase in the temperature of the reactor decreases the chemical conversion extent of the reaction. Moreover, an increase in the temperature of the reactor causes the reaction to proceed in the reverse direction, which is endothermic. Normally, in the demonstration cases for the WGS reaction, the temperature is low (e.g.,  $200\text{ }^{\circ}\text{C}$ ) where the production of  $\text{CO}_2$  is maximized while the production of  $\text{CO}$  is suppressed, however, increasing the temperature results in the promotion of the production of  $\text{CO}_2$ .

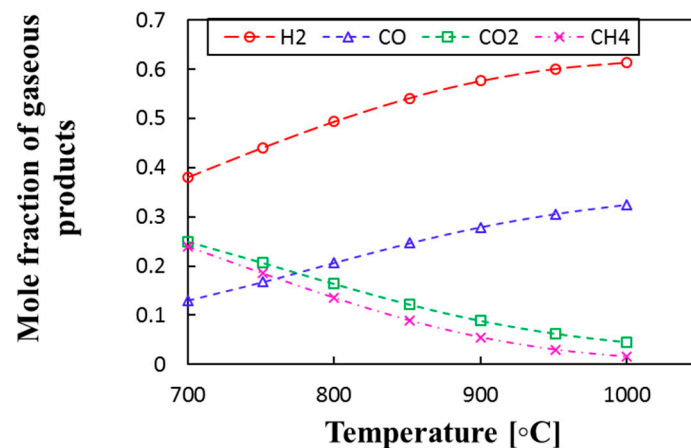


**Figure 9.** Variation of the mole fraction of the product with temperature at the reference condition for reactor  $R_2$ .

Figure 10 presents the dependence of mole fraction of gaseous products in syngas on the pressure of reactor  $R_2$  at  $T = 800\text{ }^{\circ}\text{C}$ . According to the Le Chatelier's principle, with an increase in pressure of the reactor, the reactions proceed towards the production of more gaseous products to reconcile the pressure effect. Therefore, increasing the pressure has no influence on the chemical performance of the WGS reactor [57]. However, pressurizing reactor  $R_2$  can maintain the pressure required for the syngas or hydrogen storage, which is advantageous. Therefore, there is no need to add a compressing unit to the plant, which reduces the cost significantly.

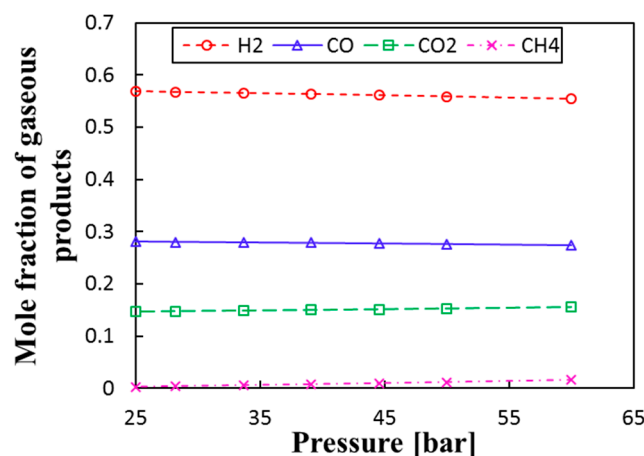


**Figure 10.** Variation of the mole fraction of the products with pressure at the reference condition in reactor  $R_2$ .

### 3.4. Biomass Composition

Figure 11a–c presents the dependence of mole fractions of gaseous products on different carbon-containing fuels.

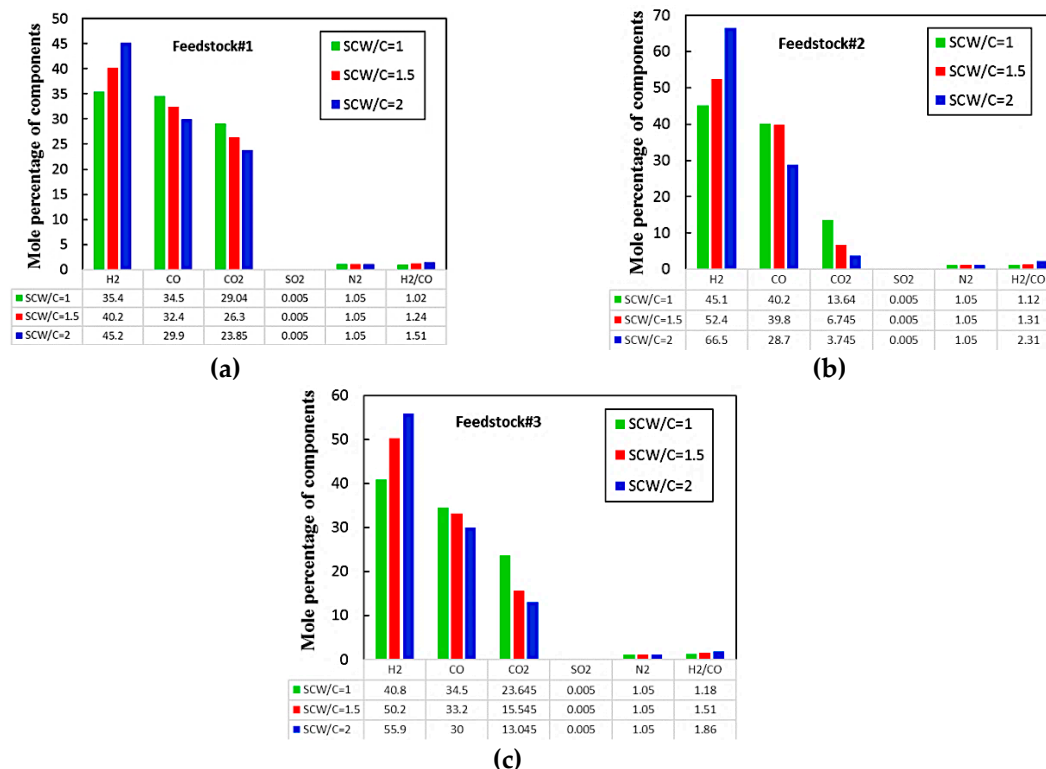


**Figure 11.** Mole percentage of components in gaseous products for different molar ratios of SCW/C and for different biomass feedstock given in Table 2 and at 900 °C (a) feedstock #1, (b) feedstock #2, and (c) feedstock #3.

As shown in Figure 11a, feedstock#1, has the lowest amount of carbon content and the highest amount of oxygen as compared with the other feedstocks. Therefore, more oxygen is available to produce carbon dioxide and a lower syngas quality ( $H_2:CO$  molar ratio) is obtained as compared with other feedstocks. For example, at  $SCW/C = 1$ , the syngas quality ( $H_2:CO$  molar ratio) is 1.02, 1.12, and 1.18, for feedstock 1, 2, and 3, respectively. It is worth noting that the low content of sulphur promotes the quality of the syngas. In addition, the lower the content of nitrogen, the higher the syngas quality ( $H_2:CO$  molar ratio). Feedstock#2, as presented in Figure 11b, has the lowest amount of oxygen content, and therefore the mole fraction of  $CO_2$  is the lowest, while the quality of syngas ( $H_2:CO$  molar ratio) of 2.31 is obtained at  $SCW/C = 2$ . Similarly, with an increase in the molar ratio of  $SCW/C$ , the mole fraction of  $H_2$  increases for all the biomass feedstocks, while it decreases for  $CO_2$  and  $CO$ . For example, for feedstock#1, with an increase in the  $SCW/C$  ratio from 1 to 2, the mole percentage of hydrogen increases from 35.4% to 45.2%, while the mole percentage of  $CO$  and  $CO_2$  decreases from 34.5% to 29.9% and 29.03% to 23.85%, respectively. This is attributed to the increase in the content of hydrogen and the suppression of reaction 3 due to the enrichment of hydrogen in the gas product. Since the obtained results are based on the equilibrium Gibbs minimization model, a series of experiments is required to validate and demonstrate the reactions and accurately justify the behaviour of the system based on the kinetic parameters.

#### 4. Conclusions

A thermodynamic assessment was conducted on a supercritical water gasification with a water–gas shift reactor to assess the potential chemical performance of the proposed concept. The following conclusions were made:

1. The addition of a water–gas shift reactor adds more control on the ratio of H<sub>2</sub>:CO and minimizes the production of CH<sub>4</sub> and CO<sub>2</sub>. For the proposed system, the quality of syngas (H<sub>2</sub>:CO molar ratio) reaches 2.1 at P = 25 bar and 850 °C and 900 °C for reactors R<sub>1</sub> and R<sub>2</sub>, respectively.
2. Pressure was found to have no influence on the chemical performance of the water–gas shift reactor. However, pressurizing reactor R2 provides the pressure required for the storage of gas and reduces the cost of post-compression of products.
3. The proposed system produces the syngas with different H<sub>2</sub>:CO ratios depending on the SCW/C and the temperature. For a given specific biomass, we found that syngas with the quality of 2.3 was produced at 900 °C and SCW/C = 2.

**Author Contributions:** Conceptualization, M.M.S.; methodology, M.M.S., M.G., M.J., and M.A.; software, M.M.S. and M.J.; validation, M.M.S. and M.J.; formal analysis, M.M.S., M.J., and M.R.S.; investigation, M.M.S., M.J., M.R.S., M.G., and M.A.; writing—original draft preparation, M.M.S., M.R.S., M.J., and M.G.; writing—review and editing, M.M.S., M.J., M.R.S., M.G., and M.A.; supervision, M.A.

**Funding:** This research received no external funding.

**Acknowledgments:** The authors acknowledge the school of Mechanical Engineering, University of Adelaide for the scientific support.

**Conflicts of Interest:** The authors declare no conflict of interest.

#### References

1. Turner, J.A. A realizable renewable energy future. *Science* **1999**, *285*, 687–689. [[CrossRef](#)] [[PubMed](#)]
2. Ogden, J.M.; Williams, R.H. *Solar Hydrogen: Moving Beyond Fossil Fuels*; World Resources Inst: Washington, DC, USA, 1989.
3. Klass, D.L. *Biomass for Renewable Energy, Fuels, and Chemicals*; Academic Press: Cambridge, MA, USA, 1998.
4. Dry, M.E. The fischer–tropsch process: 1950–2000. *Catal. Today* **2002**, *71*, 227–241. [[CrossRef](#)]
5. Gemmen, R.; Tremblay, J. On the mechanisms and behavior of coal syngas transport and reaction within the anode of a solid oxide fuel cell. *J. Power Sources* **2006**, *161*, 1084–1095. [[CrossRef](#)]
6. Adanez, J.; Abad, A.; Garcia-Labiano, F.; Gayan, P.; Luis, F. Progress in chemical-looping combustion and reforming technologies. *Prog. Energy Combust. Sci.* **2012**, *38*, 215–282. [[CrossRef](#)]
7. Jafarian, M.; Arjomandi, M.; Nathan, G.J. Thermodynamic potential of high temperature chemical looping combustion with molten iron oxide as the oxygen carrier. *Chem. Eng. Res. Des.* **2017**, *120*, 69–81. [[CrossRef](#)]
8. Jafarian, M.; Arjomandi, M.; Nathan, G.J. A hybrid solar and chemical looping combustion system for solar thermal energy storage. *Appl. Energy* **2013**, *103*, 671–678. [[CrossRef](#)]
9. Jafarian, M.; Arjomandi, M.; Nathan, G.J. A hybrid solar chemical looping combustion system with a high solar share. *Appl. Energy* **2014**, *126*, 69–77. [[CrossRef](#)]
10. Jafarian, M.; Arjomandi, M.; Nathan, G.J. The energetic performance of a novel hybrid solar thermal & chemical looping combustion plant. *Appl. Energy* **2014**, *132*, 74–85.
11. Tanner, J.; Bhattacharya, S. Kinetics of CO<sub>2</sub> and steam gasification of Victorian brown coal chars. *Chem. Eng. J.* **2016**, *285*, 331–340. [[CrossRef](#)]
12. Patra, T.K.; Sheth, P.N. Biomass gasification models for downdraft gasifier: A state-of-the-art review. *Renew. Sustain. Energy Rev.* **2015**, *50*, 583–593. [[CrossRef](#)]
13. Chan, F.L.; Tanksale, A. Review of recent developments in Ni-based catalysts for biomass gasification. *Renew. Sustain. Energy Rev.* **2014**, *38*, 428–438. [[CrossRef](#)]
14. Ge, H.; Guo, W.; Shen, L.; Song, T.; Xiao, J. Biomass gasification using chemical looping in a 25kW th reactor with natural hematite as oxygen carrier. *Chem. Eng. J.* **2016**, *286*, 174–183. [[CrossRef](#)]

15. Adánez, J.; Gayán, P.; Celaya, J.; de Diego, L.F.; García-Labiano, F.; Abad, A. Chemical looping combustion in a 10 kWth prototype using a CuO/Al<sub>2</sub>O<sub>3</sub> oxygen carrier: Effect of operating conditions on methane combustion. *Ind. Eng. Chem. Res.* **2006**, *45*, 6075–6080. [[CrossRef](#)]
16. Li, F.; Kim, H.R.; Sridhar, D.; Wang, F.; Zeng, L.; Chen, J.; Fan, L.-S. Syngas chemical looping gasification process: Oxygen carrier particle selection and performance. *Energy Fuels* **2009**, *23*, 4182–4189. [[CrossRef](#)]
17. Liao, C.; Wu, C.; Yan, Y. The characteristics of inorganic elements in ashes from a 1 MW CFB biomass gasification power generation plant. *Fuel Process. Technol.* **2007**, *88*, 149–156. [[CrossRef](#)]
18. Fan, L.; Li, F.; Ramkumar, S. Utilization of chemical looping strategy in coal gasification processes. *Particuology* **2008**, *6*, 131–142. [[CrossRef](#)]
19. Acharya, B.; Dutta, A.; Basu, P. Chemical-looping gasification of biomass for hydrogen-enriched gas production with in-process carbon dioxide capture. *Energy Fuels* **2009**, *23*, 5077–5083. [[CrossRef](#)]
20. Anheden, M.; Svedberg, G. Exergy analysis of chemical-looping combustion systems. *Energy Convers. Manag.* **1998**, *39*, 1967–1980. [[CrossRef](#)]
21. Zevenhoven-Onderwater, M.; Backman, R.; Skrifvars, B.-J.; Hupa, M. The ash chemistry in fluidised bed gasification of biomass fuels. Part I: Predicting the chemistry of melting ashes and ash-bed material interaction. *Fuel* **2001**, *80*, 1489–1502. [[CrossRef](#)]
22. Florin, N. Calcium looping technologies for gasification and reforming. In *Calcium and Chemical Looping Technology for Power Generation and Carbon Dioxide (CO<sub>2</sub>) Capture*; Woodhead Publishing: Sawston, UK, 2015.
23. Matsumura, Y.; Minowa, T.; Potic, B.; Kersten, S.R.A.; Prins, W.; van Swaaij, W.P.M.; van de Beld, B.; Elliott, D.C.; Neuenschwander, G.G.; Kruse, A. Biomass gasification in near-and super-critical water: Status and prospects. *Biomass Bioenergy* **2005**, *29*, 269–292. [[CrossRef](#)]
24. Kruse, A. Supercritical water gasification. *Biofuels Bioprod. Biorefining Innov. Sustain. Econ.* **2008**, *2*, 415–437. [[CrossRef](#)]
25. Williams, P.T.; Onwudili, J. Subcritical and supercritical water gasification of cellulose, starch, glucose, and biomass waste. *Energy Fuels* **2006**, *20*, 1259–1265. [[CrossRef](#)]
26. Withag, J.A.; Smeets, J.R.; Bramer, E.A.; Brem, G. System model for gasification of biomass model compounds in supercritical water—a thermodynamic analysis. *J. Supercrit. Fluids* **2012**, *61*, 157–166. [[CrossRef](#)]
27. Guan, Q.; Savage, P.E.; Wei, C. Gasification of alga *Nannochloropsis* sp. in supercritical water. *J. Supercrit. Fluids* **2012**, *61*, 139–145. [[CrossRef](#)]
28. Yakaboylu, O.; Albrecht, I.; Harinck, J.; Smit, K.; Tsalidis, G.-A.; Di Marcello, M.; Anastakis, K.; de Jong, W. Supercritical water gasification of biomass in fluidized bed: First results and experiences obtained from TU Delft/Gensos semi-pilot scale setup. *Biomass Bioenergy* **2018**, *111*, 330–342. [[CrossRef](#)]
29. Guo, L.; Lu, Y.; Zhang, X.; Ji, C.; Guan, Y.; Pei, A. Hydrogen production by biomass gasification in supercritical water: A systematic experimental and analytical study. *Catal. Today* **2007**, *129*, 275–286. [[CrossRef](#)]
30. Yu, D.; Aihara, M.; Antal, M.J., Jr. Hydrogen production by steam reforming glucose in supercritical water. *Energy Fuels* **1993**, *7*, 574–577. [[CrossRef](#)]
31. Yong, T.L.-K.; Matsumura, Y. Reaction kinetics of the lignin conversion in supercritical water. *Ind. Eng. Chem. Res.* **2012**, *51*, 11975–11988. [[CrossRef](#)]
32. Zhu, C.; Wang, R.; Jin, H.; Lian, X.; Guo, L.; Huang, J. Supercritical water gasification of glycerol and glucose in different reactors: The effect of metal wall. *Int. J. Hydrog. Energy* **2016**, *41*, 16002–16008. [[CrossRef](#)]
33. Reddy, S.N.; Nanda, S.; Dalai, A.K.; Kozinski, J.A. Supercritical water gasification of biomass for hydrogen production. *Int. J. Hydrogen Energy* **2014**, *39*, 6912–6926. [[CrossRef](#)]
34. Tang, H.; Kitagawa, K. Supercritical water gasification of biomass: Thermodynamic analysis with direct Gibbs free energy minimization. *Chem. Eng. J.* **2005**, *106*, 261–267. [[CrossRef](#)]
35. Castello, D.; Fiori, L. Supercritical water gasification of biomass: Thermodynamic constraints. *Bioresour. Technol.* **2011**, *102*, 7574–7582. [[CrossRef](#)] [[PubMed](#)]
36. Lu, Y.; Zhao, L.; Han, Q.; Wei, L.; Zhang, X.; Guo, L.; Wei, J. Minimum fluidization velocities for supercritical water fluidized bed within the range of 633–693 K and 23–27 MPa. *Int. J. Multiph. Flow* **2013**, *49*, 78–82. [[CrossRef](#)]
37. Sarafraz, M.M.; Jafarian, M.; Arjomandi, M.; Nathan, G.J. The relative performance of alternative oxygen carriers for liquid chemical looping combustion and gasification. *Int. J. Hydrogen Energy* **2017**, *42*, 16396–16407. [[CrossRef](#)]

38. Sarafraz, M.M.; Jafarian, M.; Arjomandi, M.; Nathan, G.J. Potential of molten lead oxide for liquid chemical looping gasification (LCLG): A thermochemical analysis. *Int. J. Hydrogen Energy* **2018**, *43*, 4195–4210. [[CrossRef](#)]
39. Sarafraz, M.M.; Jafarian, M.; Arjomandi, M.; Nathan, G.J. The thermo-chemical potential liquid chemical looping gasification with bismuth oxide. *Int. J. Hydrogen Energy* **2019**, *44*, 8038–8050. [[CrossRef](#)]
40. Salari, E.; Peyghambarzadeh, M.; Sarafraz, M.M.; Hormozi, F. Boiling heat transfer of alumina nano-fluids: Role of nanoparticle deposition on the boiling heat transfer coefficient. *Period. Polytech. Chem. Eng.* **2016**, *60*, 252–258. [[CrossRef](#)]
41. Salari, E.; Peyghambarzadeh, S.M.; Sarafraz, M.M.; Hormozi, F.; Nikkhah, V. Thermal behavior of aqueous iron oxide nano-fluid as a coolant on a flat disc heater under the pool boiling condition. *Heat Mass Transf.* **2017**, *53*, 265–275. [[CrossRef](#)]
42. Sarafraz, M.M.; Arya, A.; Nikkhah, V.; Hormozi, F. Thermal performance and viscosity of biologically produced silver/coconut oil nanofluids. *Chem. Biochem. Eng. Q.* **2017**, *30*, 489–500. [[CrossRef](#)]
43. Arya, A.; Sarafraz, M.M.; Shahmiri, S.; Madani, S.A.H.; Nikkhah, V.; Nakhjavani, S.M. Thermal performance analysis of a flat heat pipe working with carbon nanotube-water nanofluid for cooling of a high heat flux heater. *Heat Mass Transf.* **2018**, *54*, 985–997. [[CrossRef](#)]
44. Sarafraz, M.M.; Arjomandi, M. Demonstration of plausible application of gallium nano-suspension in microchannel solar thermal receiver: Experimental assessment of thermo-hydraulic performance of microchannel. *Int. Commun. Heat Mass Transf.* **2018**, *94*, 39–46. [[CrossRef](#)]
45. Guo, Y.; Wang, S.Z.; Xu, D.H.; Gong, Y.M.; Ma, H.H.; Tang, X.Y. Review of catalytic supercritical water gasification for hydrogen production from biomass. *Renew. Sustain. Energy Rev.* **2010**, *14*, 334–343. [[CrossRef](#)]
46. Chakinala, A.G.; Brillman, D.W.F.; van Swaaij, W.P.M.; Kersten, S.R.A. Catalytic and non-catalytic supercritical water gasification of microalgae and glycerol. *Ind. Eng. Chem. Res.* **2009**, *49*, 1113–1122. [[CrossRef](#)]
47. Yanik, J.; Ebale, S.; Kruse, A.; Saglam, M.; Yüksel, M. Biomass gasification in supercritical water: II. Effect of catalyst. *Int. J. Hydrogen Energy* **2008**, *33*, 4520–4526. [[CrossRef](#)]
48. Aziz, M. Integrated supercritical water gasification and a combined cycle for microalgal utilization. *Energy Convers. Manag.* **2015**, *91*, 140–148. [[CrossRef](#)]
49. Wan, W. An innovative system by integrating the gasification unit with the supercritical water unit to produce clean syngas: Effects of operating parameters. *Int. J. Hydrogen Energy* **2016**, *41*, 14573–14582. [[CrossRef](#)]
50. Wan, W. An innovative system by integrating the gasification unit with the supercritical water unit to produce clean syngas for solid oxide fuel cell (SOFC): System performance assessment. *Int. J. Hydrogen Energy* **2016**, *41*, 22698–22710. [[CrossRef](#)]
51. Li, N.; Li, Y.; Ban, Y.; Song, Y.; Zhi, K.; Teng, Y.; He, R.; Zhou, H.; Liu, Q.; Qi, Y. Direct production of high hydrogen syngas by steam gasification of Shengli lignite/chars: Remarkable promotion effect of inherent minerals and pyrolysis temperature. *Int. J. Hydrogen Energy* **2017**, *42*, 5865–5872. [[CrossRef](#)]
52. Calzavara, Y.; Jousot-Dubien, C.; Boissonnet, G.; Sarrade, S. Evaluation of biomass gasification in supercritical water process for hydrogen production. *Energy Convers. Manag.* **2005**, *46*, 615–631. [[CrossRef](#)]
53. McKendry, P. Energy production from biomass (part 1): Overview of biomass. *Bioresour. Technol.* **2002**, *83*, 37–46. [[CrossRef](#)]
54. Indrawan, N.; Thapa, S.; Bhoi, P.R.; Huhnke, R.L.; Kumar, A. Engine power generation and emission performance of syngas generated from low-density biomass. *Energy Convers. Manag.* **2017**, *148*, 593–603. [[CrossRef](#)]
55. Ong, Z.; Cheng, Y.; Maneerung, T.; Yao, Z.; Tong, Y.W.; Wang, C.H.; Dai, Y. Co-gasification of woody biomass and sewage sludge in a fixed-bed downdraft gasifier. *AIChE J.* **2015**, *61*, 2508–2521. [[CrossRef](#)]
56. Zhai, Y.; Peng, C.; Xu, B.; Wang, T.; Li, C.; Zeng, G.; Zhu, Y. Hydrothermal carbonisation of sewage sludge for char production with different waste biomass: Effects of reaction temperature and energy recycling. *Energy* **2017**, *127*, 167–174. [[CrossRef](#)]
57. Bustamante, F.; Enick, R.; Rothenberger, K.; Howard, B.; Cugini, A.; Ciocco, M.; Morreale, B. Kinetic study of the reverse water gas shift reaction in high-temperature, high pressure homogeneous systems. *Fuel Chem. Div. Prepr.* **2002**, *47*, 663–664.

